

Article

Analysis of Long-Term Prestress Loss in Prestressed Concrete (PC) Structures Using Fiber Bragg Grating (FBG) Sensor-Embedded PC Strands

Sung-Tae Kim ¹, Young-Soo Park ¹, Chul-Hwan Yoo ¹, Soobong Shin ² and Young-Hwan Park ^{1,*} 

¹ Department of Structural Engineering Research, Korea Institute of Civil Engineering and Building Technology, Goyang 10223, Korea; esper009@kict.re.kr (S.-T.K.); youngsoopark@kict.re.kr (Y.-S.P.); jahad1010@kict.re.kr (C.-H.Y.)

² Department of Civil Engineering, Inha University, Incheon 22212, Korea; sbshin@inha.ac.kr

* Correspondence: yhpark@kict.re.kr; Tel.: +82-31-910-0126

Abstract: This study aims to develop a prestressed concrete steel (PC) strand with an embedded optical Fiber Bragg Grating (FBG) sensor, which has been developed by the Korea Institute of Civil Engineering and Building Technology since 2013. This new strand is manufactured by replacing the steel core of the normal PC strand with a carbon-fiber-reinforced polymer (CFRP) rod with excellent tensile strength and durability. Because this new strand is manufactured using the pultrusion method, which is a composite material manufacturing process, with an optical fiber sensor embedded in the inner center of the CFRP Rod, it ensures full composite action as well as proper function of the sensor. In this study, a creep test for maintaining a constant load and a relaxation test for maintaining a constant displacement were performed on the proposed sensor-type PC strand. Each of the two tests was conducted for more than 1000 h, and the long-term performance verification of the sensor-type PC strand was only completed by comparing the performance with that of a normal PC strand. The test specimens were fabricated by applying an optical fiber sensor-embedded PC strand, which had undergone long-term performance verification tests, to a reinforced concrete beam. Depending on whether grout was injected in the duct, the specimens were classified into composite and non-composite specimens. A hydraulic jack was used to prestress the fabricated beam specimens, and the long-term change in the prestress force was observed for more than 1600 days using the embedded optical fiber sensor. The experimental results were compared with the analytical results to determine the long-term prestress loss obtained through finite-element analysis based on various international standards.



Citation: Kim, S.-T.; Park, Y.-S.; Yoo, C.-H.; Shin, S.; Park, Y.-H. Analysis of Long-Term Prestress Loss in Prestressed Concrete (PC) Structures Using Fiber Bragg Grating (FBG) Sensor-Embedded PC Strands. *Appl. Sci.* **2021**, *11*, 12153. <https://doi.org/10.3390/app112412153>

Academic Editor: José Correia

Received: 24 November 2021

Accepted: 14 December 2021

Published: 20 December 2021

Keywords: bridge; prestressed concrete; PC strand; optical sensor; prestressing force management

Publisher's Note: MDPI stays neutral with regard to jurisdictional claims in published maps and institutional affiliations.



Copyright: © 2021 by the authors. Licensee MDPI, Basel, Switzerland. This article is an open access article distributed under the terms and conditions of the Creative Commons Attribution (CC BY) license (<https://creativecommons.org/licenses/by/4.0/>).

1. Introduction

Prestressed concrete (PC) structures are widely used for most concrete structures because of their advantage with respect to the increased compression efficiency of concrete and the improved cracking characteristics when using PC steel strands. In general, cracks mainly occur in the area in which the tensile force acts because the tensile strength of concrete is significantly smaller than the compressive strength. PSC is an efficient structure that applies a compressive force to the region in which the tensile force is applied to remove some of the tensile stress generated in the concrete by external loads. The advantages of PC, such as a reduction in the cross-sectional area and the amount of reinforcement, have led to the construction of numerous PC structures. As more than 100 years have passed since the development of PC structures, the number of PC structures undergoing aging is increasing tremendously, with an increased importance given to maintenance through monitoring of the structures. Because the most typical method of applying prestress force in such PC is to use a PC strand, the long-term performance of this PC strand is a critical factor.

In general, when introducing a prestress force into a structure using a PC strand, the prestress force is calculated based on the hydraulic change and the extension of the hydraulic jack, as shown in Figure 1. Therefore, a separate measurement method is required to examine the residual prestress force after removing the hydraulic jack. The lift-off test is often used [1–3] and is a method that is employed to install a load cell, a displacement meter, and a hydraulic jack on the strand and to calculate the prestress force of the strand using the relationship between the force applied to the load cell and the displacement measured with the displacement meter. Although the process is simple and accurate, it is difficult to apply this method to structures in service, as it involves separate hydraulic equipment and excessive hydraulic pressure may, thus, be introduced.

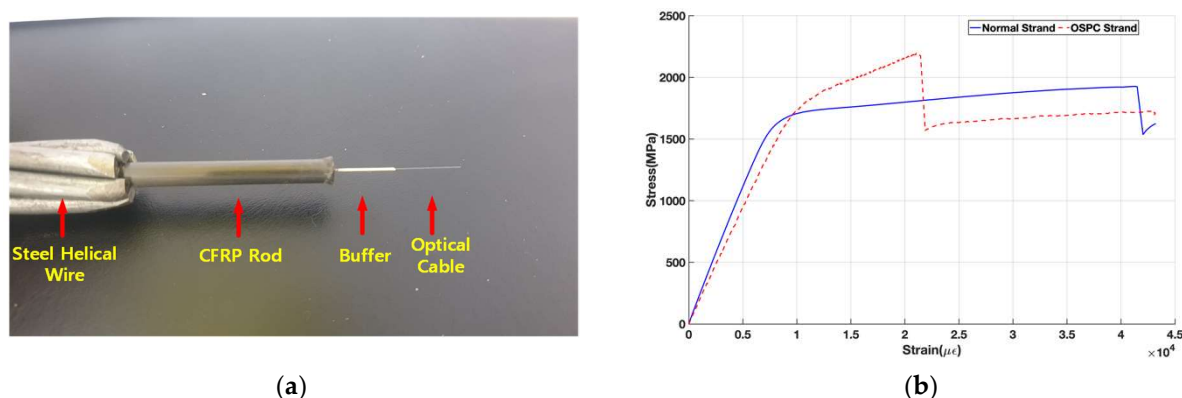


Figure 1. Appearance of the OSPC strand and tensile strength test results (a) Fabricated OSPC strand, (b) Tensile strength test results.

After examining the prestress force in the above manner and then removing the hydraulic jack, there are not many ways to manage the prestress force. Therefore, the maintenance of the prestress force tends to be neglected in PC bridges in the absence of a means to check the prestress force, and leakage may occur, owing to voids in the grout in the duct and cracks in the concrete around the installed strands, leading to the corrosion of the strands and even to the collapse of bridges in severe cases. Table 1 below shows examples of bridges showing severe corrosion of prestressed members and anchorages, as well as bridge collapse accidents that have occurred since 2000.




The conventional methods used for measuring prestress force include traditional methods such as attaching a gauge directly to the outside of a strand and installing a load cell at the end. There has also been a recent approach to estimating the prestress force based on the relationship between the magnitude of the tension force and the magnetic field variation rate, which is calculated using an electromagnetic (EM) sensor or a magnetic flux leakage (MFL) sensor [7,8]. In addition, methods for measuring the prestress force or tracking damaged areas by applying an acoustic emission (AE) sensor using acoustic effects are being developed [9,10].

As most structures tend to have several PC strands applied to one duct, an externally attached sensor is associated with problems such as the need for a method to protect the sensor area and to manage the measurement line. The magnetic field or acoustic-effect-based sensors are not commonly used, as they require initial measurements, and each manufacturer employs different analysis methods for the large amount of accumulated data. Therefore, it is difficult to find a simple and stable method for long-term measurement [11,12].

This study attempted to use a PC strand with an embedded optical Fiber Bragg Grating (FBG) sensor, which has been developed by the Korea Institute of Civil Engineering and Building Technology since 2013 and evaluated the long-term performance of the strand by performing creep and relaxation tests. The trend of long-term prestress loss of each member was examined by applying optical sensor PC (OSPC) strands to the PSC beam

specimens, classified as composite and non-composite, to which the prestress force was applied [13–15]. Furthermore, a finite-element analysis was performed on beam specimens with the same dimensions to obtain the analytical results for the long-term prestress loss by applying ACI, CEB-FIP, and KS standards and the validity according to each criterion was evaluated by comparing the analytical results with the long-term prestress force data collected by the optical fiber sensor. Based on these results, this study aims to provide basic data on long-term prestress loss, which is useful for the maintenance of PSC structures.

Table 1. Examples of prestressed member damage and bridge collapse.

Bridge	Year	Patterns	Photo of Destruction
Mid bay bridge [4]	2000	Corrosion of prestressed members and anchorages	
Jeongneungcheon viaduct [5]	2016	Corrosion and fracture of prestressed members	
Morandi bridge [6]	2018	Bridge collapse due to the corrosion of prestressed members and anchorages	

2. OSPC Performance Verification

2.1. Short-Term Performance Verification—Prestress-Force Management Status and OSPC

A stable long-term measurement method to overcome the disadvantages listed above is therefore required to manage the prestress force of a PC structure. It is desirable to avoid attaching the sensor to the outside of the strand for the protection of the sensor from external factors and to use a sensor that is easy to install and to manage the connection line. This study was conducted using a PC strand with an embedded FBG sensor developed by the Korea Institute of Civil Engineering and Building Technology (optical sensor PC strand; OSPC). The OSPC strand was manufactured by producing a core wire embedded in carbon-fiber-reinforced polymer (CFRP) containing an optical fiber with FBG that could perform measurements and replacing the core wire of a normal stand with the produced core wire. The sensor was located inside the core wire and moved together with the strand to provide a high level of accuracy while exhibiting excellent durability, owing to the use of the optical fiber. Because the FBG sensor could be deployed in several places in the core wire, it was possible to monitor the prestress force on each part inside the strand [16]. Figure 1 shows the appearance of the developed OSPC strand and the tensile test results.

The maximum tensile strength of the OSPC strand was about 2200 MPa, and the yield strength was also higher than that of a normal PC strand. Nevertheless, the modulus of elasticity was about 195 GPa, which was lower than the tensile strength of 200 GPa of a normal PC strand. Although the reliability of the prestress force measurement of the OSPC strand was verified by KIM et al., it was a study that aimed to determine the reliability of short-term prestress force measurement, with no verification of the long-term performance. Therefore, in this study, strand specimens were produced for the creep and relaxation tests conducted inside a laboratory equipped with a constant temperature and humidity

function that could meet the conditions of constant temperature and humidity. After the long-term performance of the OSPC strand was verified, it was installed in a concrete beam specimen and introduced with the prestress force equivalent to the design prestress force to examine the change in prestress force over a long period of time while being exposed to external environments with varying temperatures and humidities.

2.2. Long-Term Performance Verification—Creep Test

A creep test was performed to verify the long-term performance of the OSPC strand alone. For comparison, the test was performed on a normal PC strand as well as the OSPC strand. The creep test examined the change in strain under constant stress, and it was crucial to apply a constant load to the OSPC strand throughout the test. To enable this, this study devised a load amplifier, as shown in Figure 2, and applied it to the experiment. The load amplifier used the principle of the lever and was designed to use a steel plate as a weight and to apply the amplified load to the specimen according to the distance ratio of the lever. Depending on the length ratios of a to b and c to d in Figure 2a, a load equivalent to about 80 times the actual weight was applied to the specimen. For accurate testing, monoheads were used at both ends of the specimen to create anchorages and were installed in the load amplifier. The strain was measured with an optical fiber sensor in the OSPC strand, and an electrical resistance strain sensor attached to the surface of the outer wire was used. In addition, to measure the relative slip between the core wire and the outer wire, a 10-mm displacement gauge was installed at the upper and lower parts of the specimen, and a load cell was installed to measure the change in the load. The load introduced by the load amplifier was about 175 kN, and data were obtained by performing measurements with each sensor while carrying out the test for more than 1000 h.

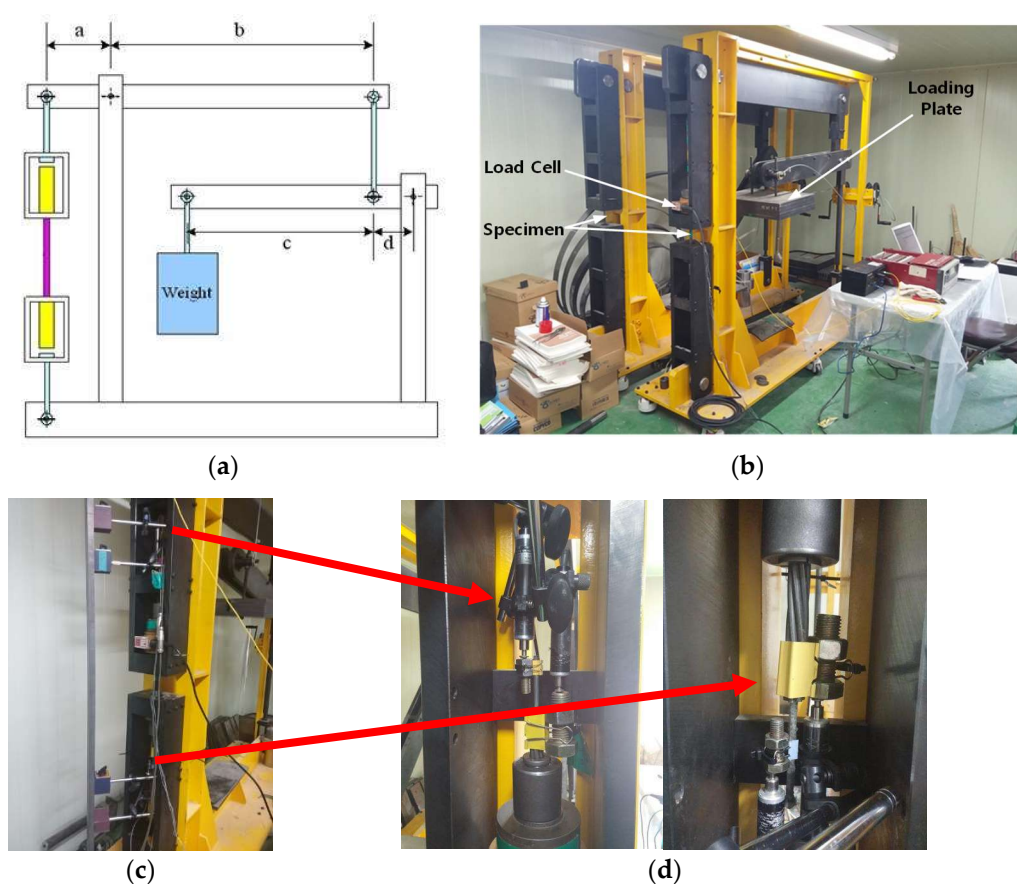


Figure 2. Creep test (a) Load amplifier, (b) Creep test, (c) Installation of sensor, (d) Upper and lower displacement meters.

Figure 3 shows the relative displacement–time curve, which is one of the creep test results of the normal PC and OSPC strands. The relative displacement was obtained by subtracting the displacement of the outer wire, located outside, from the displacement of the core wire, located in the center of the strand. The relative displacement of the OSPC strands ranged from about 0.3 mm to 1.6 mm at the beginning of loading in the upper and lower parts. The length of the specimen used in the creep test was very short, and the relative displacement varied for the normal PC strand and the OSPC strand, depending on the installation condition of the anchorage before loading. However, both strands showed a tendency to decrease the amount of change in relative displacement as the load was continuously applied over time. After a certain period of time, there was only a difference in the amount of change in the initial relative slip amount, with almost no subsequent change being observed after a certain period of time.

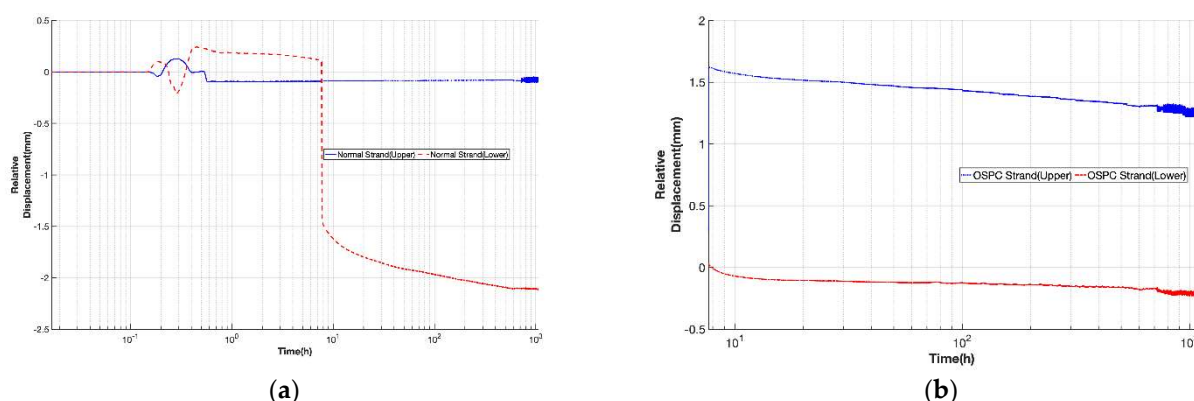


Figure 3. Creep test results—relative displacement (a) Normal PC Strand, (b) OSPC Strand.

Figure 4 shows a comparison of the strain–time curves of the normal PC and OSPC strands. While the change in strain was observed somewhat in the initial stage of loading, there was a section where it gradually stabilized over time. The abrupt change seen in the middle of the curve indicated the difference in the condition from the initial condition in the constant-temperature and constant-humidity (CTCH) chamber, owing to a power outage that occurred during the test. The CTCH chamber was repaired to continue with the test. This changed the temperature inside the laboratory for a certain period of time, and such a change in temperature resulted in a change in the strain of the specimen. After the laboratory temperature was normalized, the strain returned to the original pattern for both the normal PC and OSPC strands. After examining the change in strain of the OSPC strand under the load condition for more than 1000 h after the load was introduced, almost the same pattern was observed as in the normal PC strand. Therefore, the OSPC strand developed in this study showed high reliability measurement performance.

2.3. Long-Term Performance Verification–Relaxation Test

In order to verify the long-term performance of the OSPC strand, a relaxation test was performed in addition to the creep test. The relaxation test, which examined the change in the load under the condition with the displacement kept constant, was performed according to the test method of KS D 7002 [17]. The loading rate was (200 ± 50) N/mm² per min, and the load corresponding to 70% of the minimum value of the tensile load was applied and maintained for (120 ± 2) s. The decrease in load was measured while maintaining the distance between the anchorages for 1000 h. The final relaxation value was expressed as a percentage value for the reduced load with respect to the original load.

Figure 5 shows a schematic diagram of the test apparatus. The specimen was designed to be mounted on a rigid steel frame to prevent deformation, and the amount of change in the load was measured through a load cell. Both ends of the specimen were fixed using a mono anchorage each, and the specimen was prestressed with a hydraulic jack. When a

short strand was prestressed using a hydraulic jack, a significant amount of instantaneous loss occurred depending on the wedge slip amount and the performance of the hydraulic jack. Therefore, a hydraulic nut was installed between the frame and the load cell to recover the loss immediately after prestressing. The prestress force was first introduced by the hydraulic jack, and the hydraulic nut was used to meet the target load in order to compensate for the immediate loss caused by the removal of the hydraulic jack. The normal PC strand to be compared was SWPC7BL, with a tensile load of 261 kN, and a 70% load at 182.7 kN was applied to the specimen in this study. After prestressing to 182.7 kN and maintaining the load for 120 s, the amount of load reduction and change in strain over 1000 h were examined. Furthermore, strain sensors were attached to both sides of the steel frame in preparation for a case in which the load was reduced in the steel frame. Figure 6 shows the introduction of a load through a mono prestressing jack and a picture of the experiment.

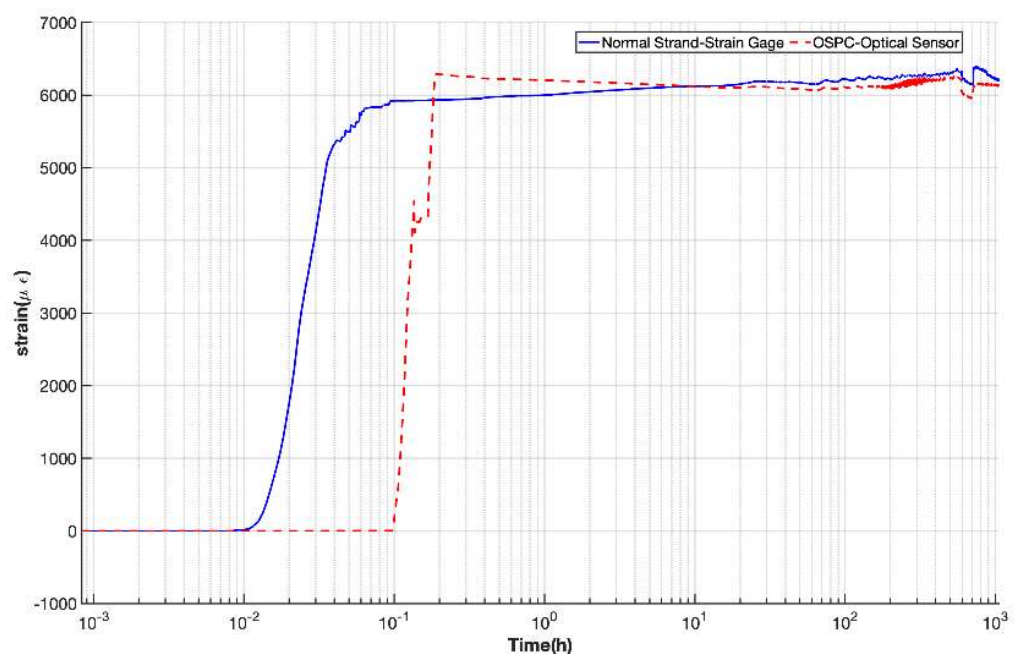


Figure 4. Creep test results—change in strain.

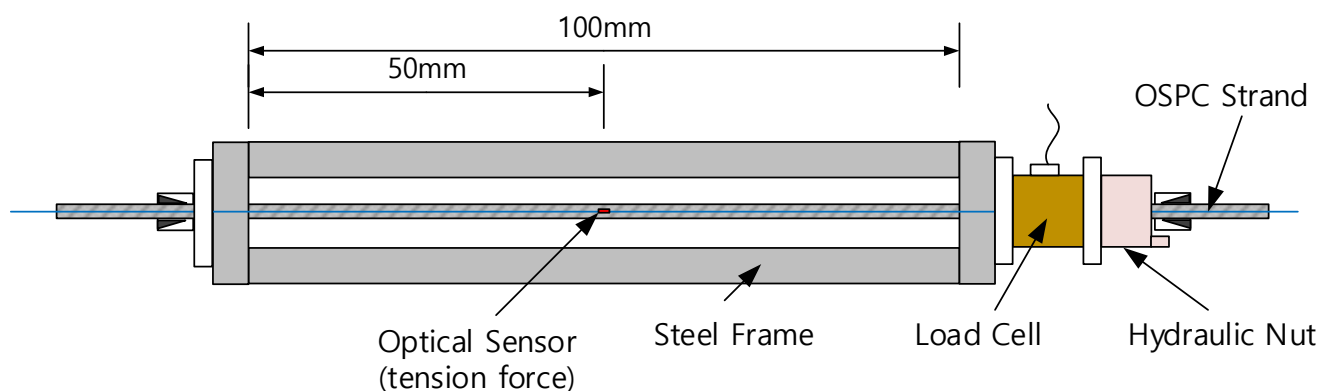


Figure 5. Relaxation test simulation.

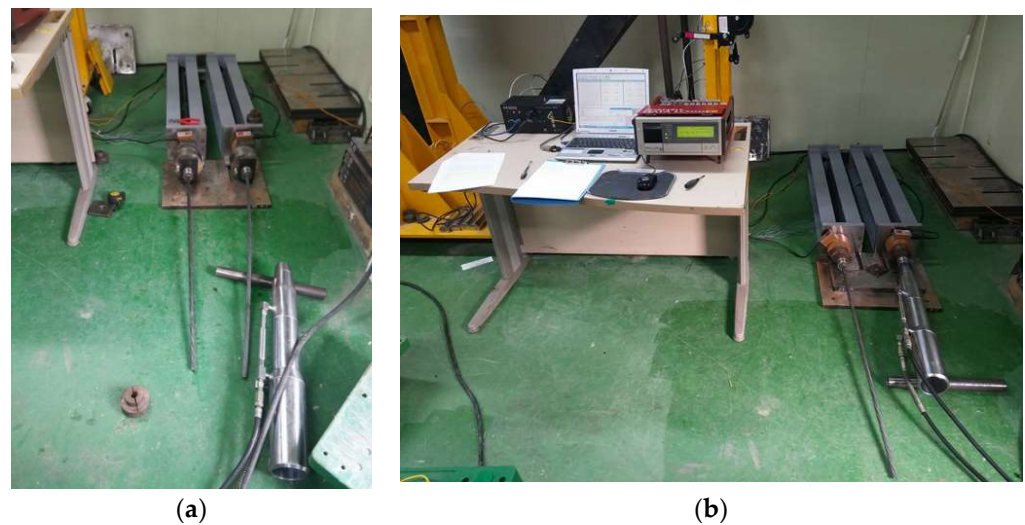


Figure 6. View of the relaxation test (a) Load introduction, (b) View of test.

Figure 7a shows the change curve of the load decrease with time for the normal PC and OSPC strands. In the figure, the degrees of load reduction, compared to the initial loads, were about 5.75 kN for the normal PC strand and about 5.25 kN for the OSPC strand. The initial loads were 180.50 kN for the general strand and 182.70 kN for the OSPC strand, which were about 3.19% and 2.87%, respectively, when calculated as a ratio. These results indicated that the relaxation performance of the OSPC strand was higher than that of the normal PC strand. However, such a load reduction did not satisfy the standard as it exceeded the standard value of 2.5% for normal low relaxation strands. Nonetheless, this value did not consider the load reduction in the steel frame. With respect to the strain reduction in the steel frame shown in Figure 7b, there was a difference in strain owing to temperature change over time, with a reduction of about 5 to 10 $\mu\epsilon$ being observed. Considering the dimension of the steel frame of 150 mm \times 75 mm \times 6.5 mm \times 10 mm with a cross-sectional area of 2371 mm², the load was about 1.2 to 2.4 kN. Because the frame was installed on both sides, the load reduction could be seen as about 2.4 to 4.8 kN. Considering the load reduction in the frame calculated in this way, the load reduction for the normal PC strand ranged from 0.95 to 3.35 kN, and the load reduction for the OSPC strand was 0.45 to 2.85 kN. Calculated as a ratio, it was about 0.53% to 1.86% for the normal PC strand and about 0.25% to 1.56% for the OSPC strand, with both strands satisfying the standard of 2.5% for low relaxation strands. Therefore, the OSPC strand demonstrated a relaxation performance equivalent to or higher than that of a normal PC strand, satisfying the standard, which indicated that it had sufficient applicability to actual structures.

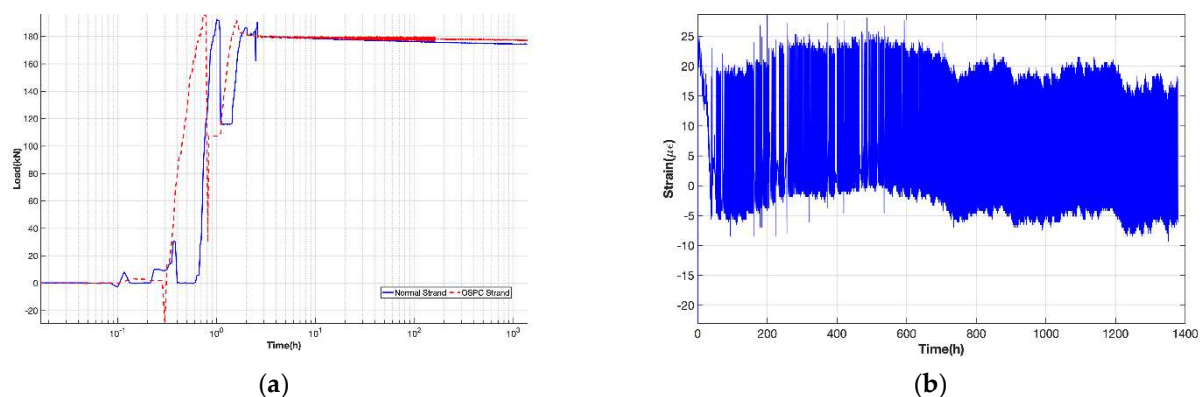


Figure 7. Relaxation test results (a) Prestress force–time changes, (b) Strain–time changes (steel frame).

2.4. Fabrication of PSC Beam Specimens

After the long-term performance verification of the strand specimens was completed, the beam specimens were fabricated to examine the behavior of OSPC strands installed in actual concrete structures. The dimensions of the specimens were based on a cross section of 300 mm in width \times 520 mm in height at the center, and the dimensions were 300 mm in width \times 600 mm in height at the support, considering the anchorage. As shown in Figure 8, the main reinforcement bars and strands were arranged inside the specimen, and the effective depth of the tendon was 460 mm. The strands were divided into composite and non-composite specimens according to the attachment method, with three strands being arranged for each specimen, and one of them was replaced with an OSPC strand. Figure 9 shows the production of the specimen and the introduction of the prestressing force. If the wavelength data measured by the optical fiber sensor of OSPC Strand were converted into a prestress force, the maximum prestress force was 184.1 kN for the composite specimen and 179.5 kN for the non-composite specimen. A total of six specimens were produced in combination with specimens for different purposes, but only the results of specimens classified as composite and non-composite specimens were used in this study.

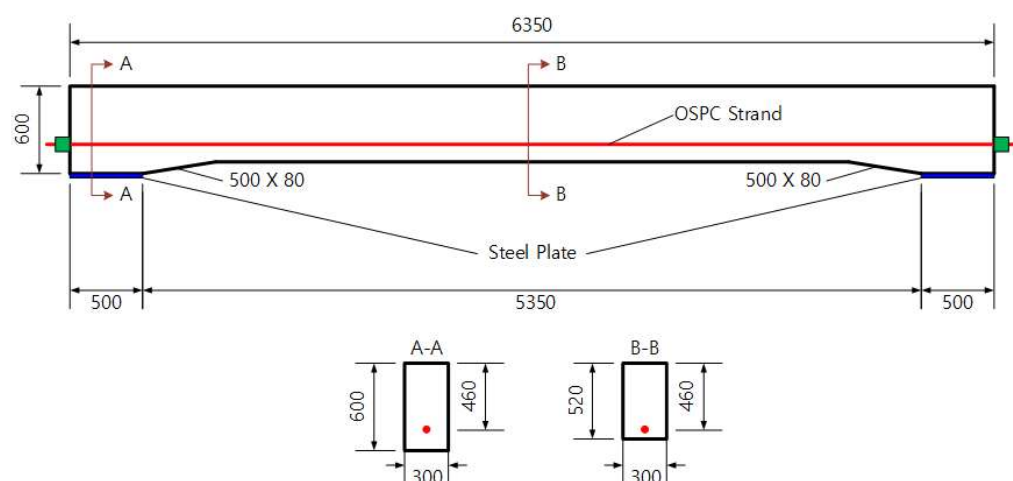


Figure 8. Dimensions and appearance of the long-term performance test specimens.

The changes in prestressing force were observed for about 1600 days in the specimens after prestressing and preparation for long-term measurement. The place where the specimen was located was an area that experiences severe temperature changes, and the range of temperature change over the four seasons was about 40 °C. The long-term measurement started around December when the temperature was low, and the change in the wavelength of light emitted from the optical fiber sensor due to the change in temperature according to the seasons was converted into a prestress force, as shown in Figure 10 below. The process of converting the optical wavelength value of the optical fiber sensor into a prestress force was applied as in the study by Seongtae Kim et al. [18]. As shown in Figure 11, there was a slight difference in the wavelength values of the optical fiber sensors in the composite and non-composite specimens, but the change was in line with the trend of seasonal temperature change.

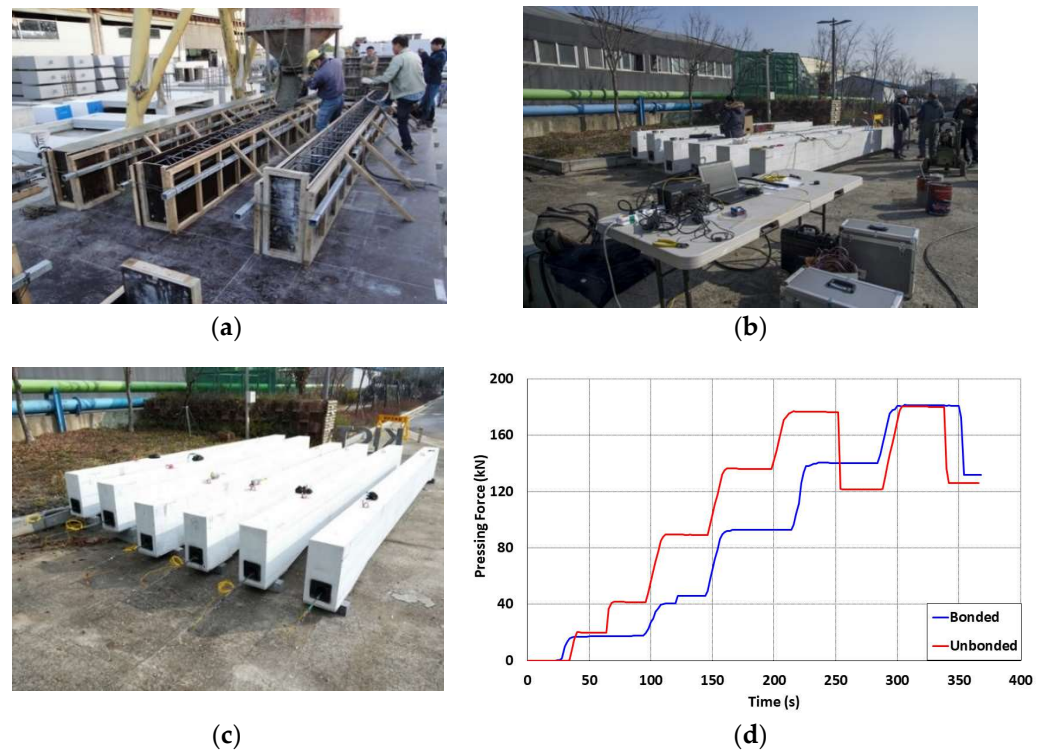


Figure 9. Fabrication and prestressing of long-term performance test specimens (a) Fabrication of specimens, (b) Prestressing and measurement, (c) Fabricated specimens, (d) Prestressing graph.

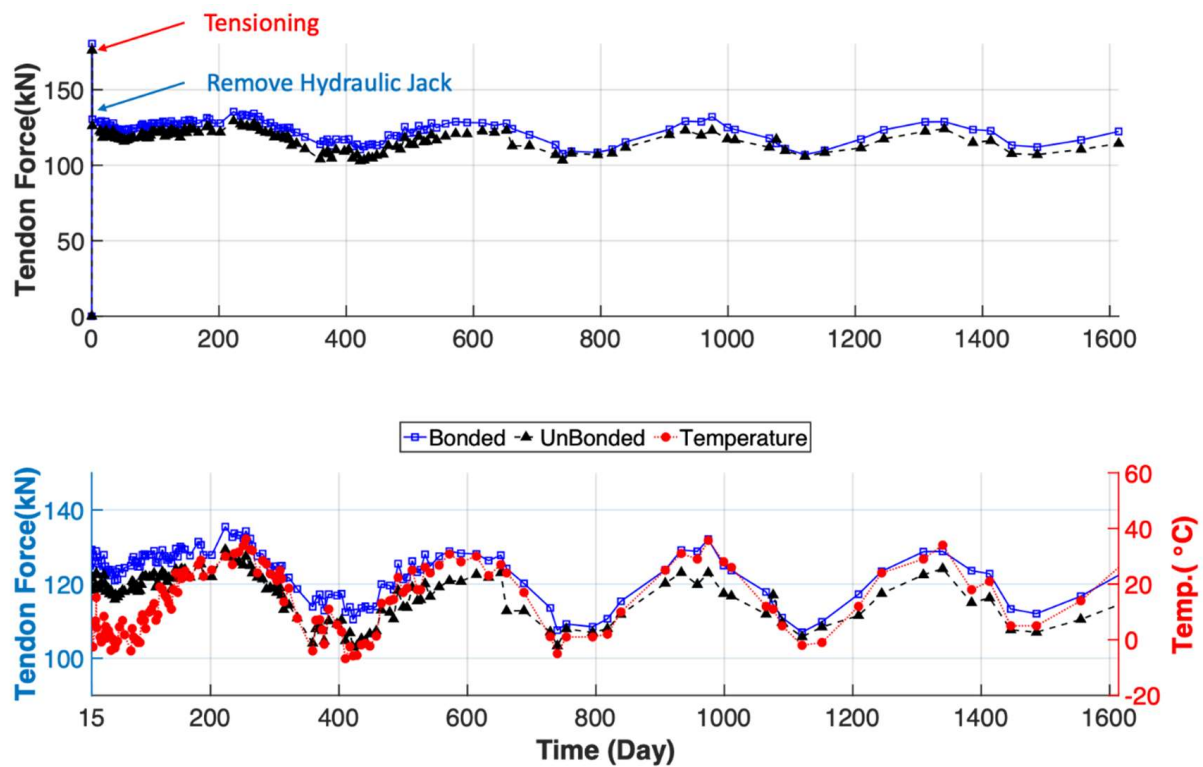


Figure 10. Change in prestress force according to temperature.

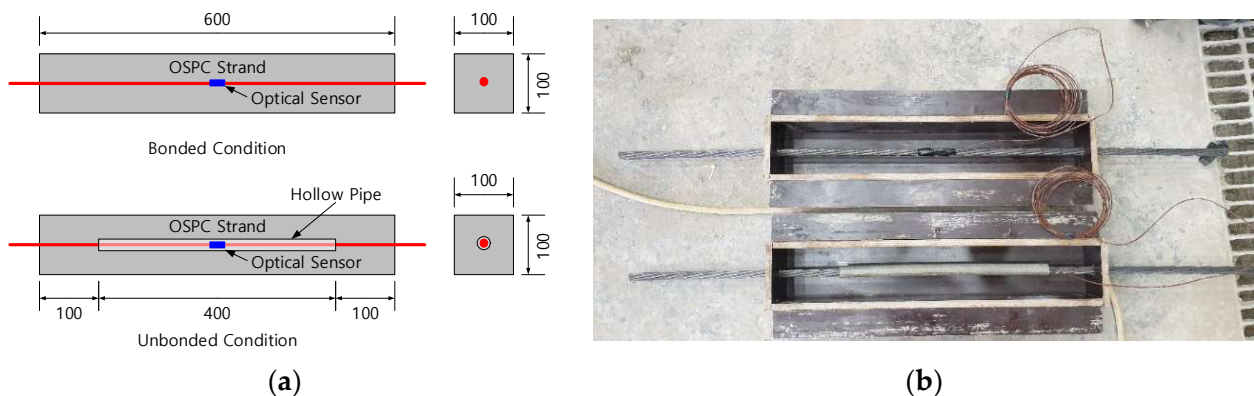


Figure 11. Dimensions of specimens and their production (a) Dimensions and appearance of specimens, (b) Fabrication of specimens.

2.5. Experiment for Temperature Compensation—Calculation of Thermal Expansion Coefficient and Data Analysis

The optical fiber sensor has excellent advantages in terms of its accuracy and durability, but it also has a disadvantage in terms of being vulnerable to temperature change. Therefore, temperature compensation is absolutely necessary where an optical fiber sensor is used. The OSPC strand behaved with materials with various coefficients of temperature expansion as it was a structure that was combined not only with the CFRP rod but also with the steel outer wire outside the strand, finally forming a composite structure with poured concrete. Therefore, this study attempted to extract only the pure change in prestress force in OSPC through a separate thermal calibration experiment. For the experiment for thermal calibration, composite and non-composite concrete beams were fabricated to match the conditions as similar as possible to the beam specimens fabricated for long-term performance verification. Figure 11 below shows the dimensions of the specimens and the production.

A chamber capable of temperature and humidity control was used for the temperature compensation experiment. In order to minimize the effects other than temperature change, a Teflon sheet with a small coefficient of friction was laid on the floor, and the test objects were placed on it to perform the experiment. Figure 12 shows the installation and measurement of a specimen in the temperature chamber. The temperature was maintained at 50 °C for 1 h, then lowered to −15 °C for 60 min, maintained at −15 °C for 60 min, and then increased to 50 °C for 60 min, where the humidity was fixed at 0%, and the temperature inside and outside the specimen and the strain of the OSPC strand were measured by repeating the same temperature pattern four times.



Figure 12. View of temperature-compensation experiments (a) Installation of specimen, (b) View of measurement.

Figure 13 shows the temperature change measured by the thermocouples installed inside and outside the specimens and the change in strain calculated by the wavelength value of the optical fiber sensors, measured in the composite and non-composite specimens. As shown in the figure, the thermal expansion coefficient of the composite specimens in which the entire OSPC strand was embedded in concrete was about $17.266 \mu\epsilon/^\circ\text{C}$. This was a slightly smaller value than the sum of the thermal expansion coefficients of the steel and optical fiber used for the normal concrete and PC strand. The thermal expansion coefficient of the optical cable may have been almost consumed, owing to the influence of the CFRP rod, with a thermal expansion coefficient close to zero, thereby being mainly affected by the thermal expansion coefficient of the steel outer wire and the concrete surrounding the CFRP rod. On the other hand, for the non-composite specimen in which the middle part formed a tube, the thermal expansion coefficient was about $9.933 \mu\epsilon/^\circ\text{C}$. Compared to the composite specimen, the behavior with respect to temperature did not show a constant pattern, but the thermal expansion coefficient was somewhat smaller than that of the composite specimen, owing to the existence of the non-composite section in the hollow tube.

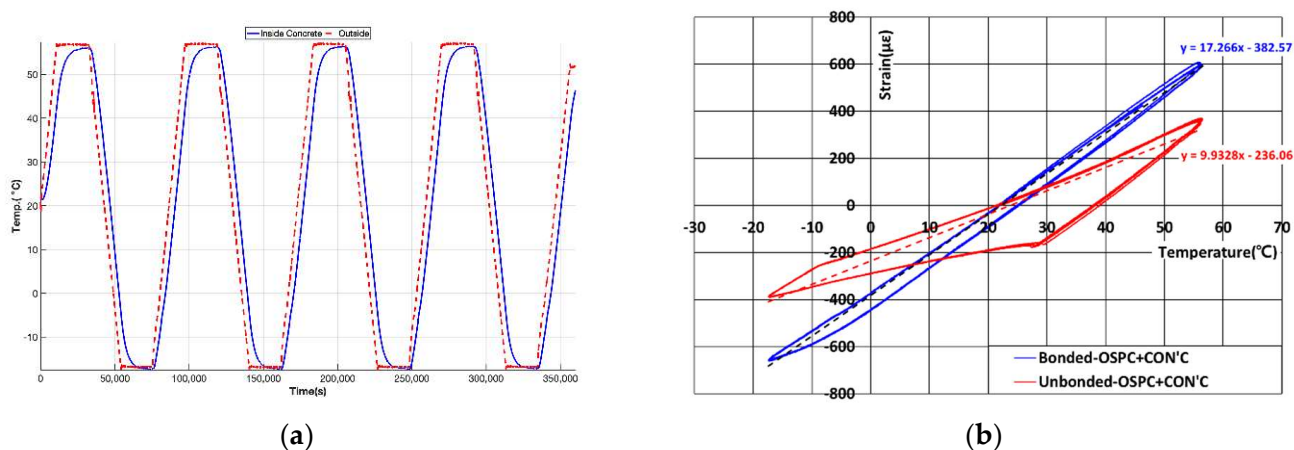


Figure 13. Results of temperature-compensation experiments (a) Temperature changes, (b) Strain-temperature changes.

Figure 14 below shows the results obtained by applying the thermal expansion coefficients calculated in the above thermal expansion coefficient experiment to the actual long-term prestress force-loss data to remove the amount of change due to heat.

As shown in Figure 15, the range of change in prestress force was significantly reduced in the upper and lower parts after removing the change in prestress force according to temperature. Hyunjong Seong et al. [19]. developed a ground anchor with a built-in optical fiber sensor and conducted a study to calculate the temperature compensation coefficient. Jianping He et al. [20]. conducted a study that analyzed the effect of temperature using a strand with a built-in optical fiber sensor similar to this study. As such, in the optical fiber sensor, the measurement data were significantly affected by the temperature change, and the effect of temperature was not considered when carrying out the finite-element analysis below for the long-term prestress loss according to the design standards in each country. Therefore, it is absolutely necessary to exclude the effect of temperature from the long-term prestress force change data in this study.

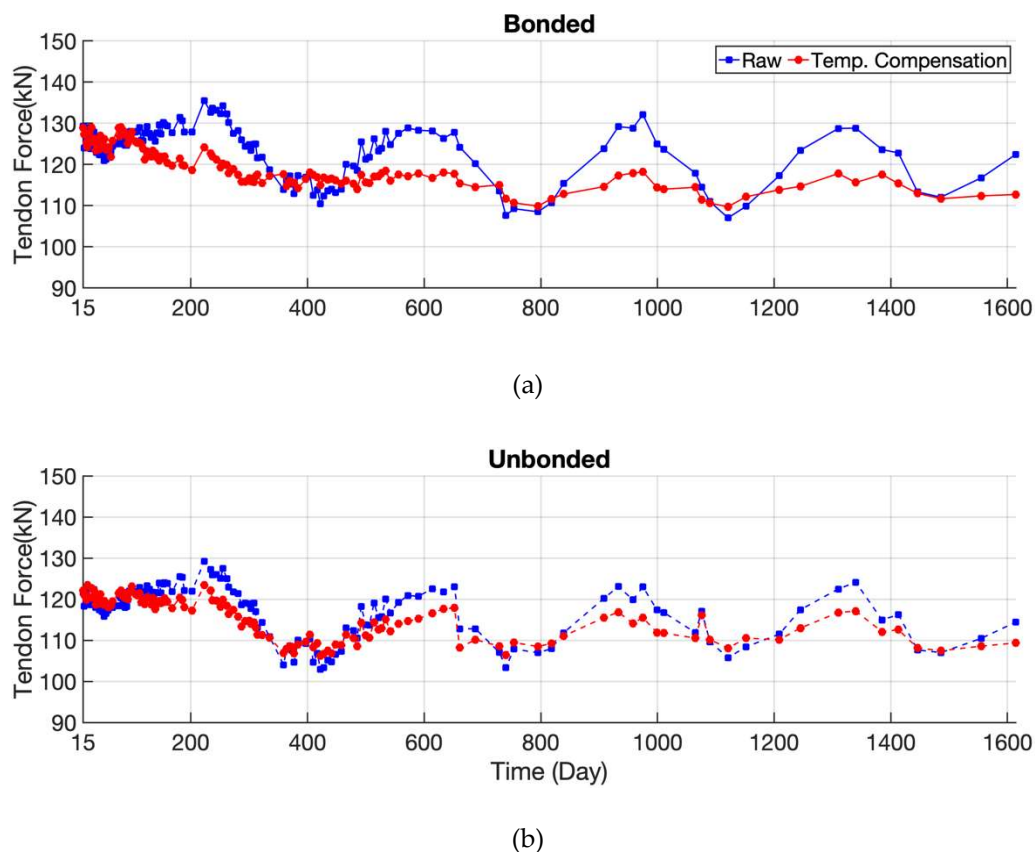


Figure 14. Change in prestress force without the influence of temperature (a) in bonded condition, (b) in unbonded condition.

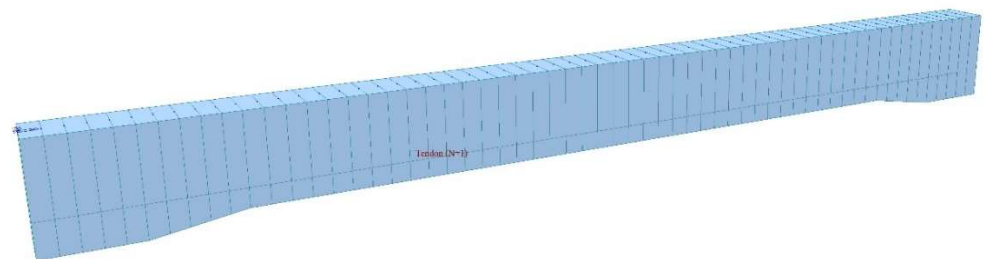


Figure 15. Modeling for finite-element analysis.

3. Finite-Element Analysis and Interpretation

In order to analytically verify the change according to the long-term prestress loss of the beam specimen installed with the OSPC strand, a finite-element model was prepared, as shown in Figure 15. MIDAS CIVIL 2020 (Seongnam, South Korea), which is a general-purpose structural analysis program, was used for finite-element analysis, and beam elements were used for modeling.

Modeling was conducted using the dimensions based on the shape of the finished specimen and the values from the compressive strength test results. Time-dependent materials required for long-term time history analysis, such as creep and shrinkage, were applied in accordance with CEB-FIP (2010), Korea Standard (2015), and ACI 318-02 (2002), the standards of each country embedded in the MIDAS program. With respect to the relaxation coefficient, the widely used equation developed by Magura [21] was applied to MIDAS, and it was entered as the value for a low relaxation strand. The curvature friction coefficient was not considered, and the wobble friction coefficient was considered to be 0.0066 (1/m). Both composite and non-composite specimens were considered, and the slip amount of the fixing unit was defined as 6 mm. The initial prestress force was 180.6 kN,

and the change in the prestress force for about 1600 days was analyzed considering the construction sequences. The prestress force acting on the tendon was analyzed for each construction phase, and the analysis was carried out by dividing it based on regulations and the composite/non-composite status, as shown in Figure 16. The arrangement of the strands was modeled using straight lines at the same location as each OSPC strand installed in the specimen. Table 2 below summarizes the main input values for each criterion applied to the finite-element analysis.

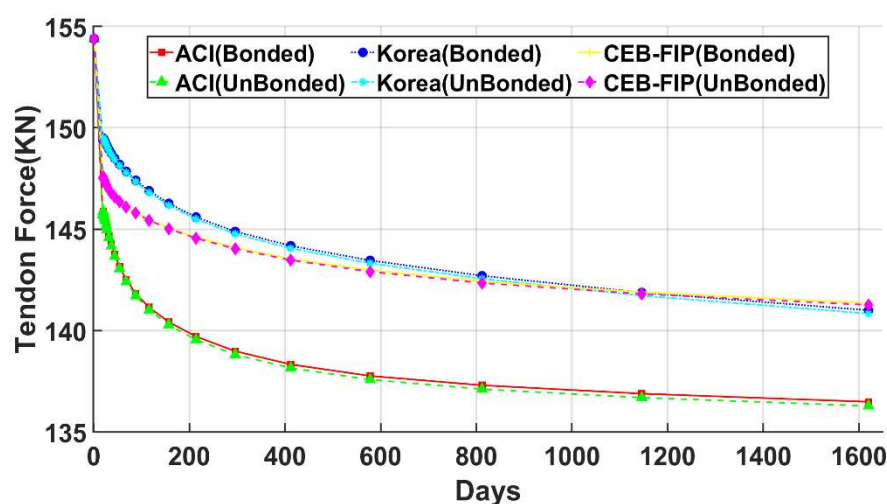


Figure 16. Analytical results for long-term prestress loss.

Table 2. Input values for finite-element analysis.

Division	ACI (Compressive Strength Coefficient)	KS (Compressive Strength Coefficient)	CEB-FIP (Cement Coefficient)
Coefficient	a:4.5, b:0.95	a:4.5, b:0.95	N,R:0.25
Applied compressive strength (MPa)	70 (compressive strength test result)		
Type of cement	Ordinary Portland Cement		

There was no significant difference in the long-term prestress loss between the composite and non-composite specimens regarding each criterion applied to the analysis. Because KS had little difference compared to CEB-FIP, the difference was even smaller regarding these two sets of standards. However, the analytical results showed a difference in terms of the change in the prestress loss in the initial stage after prestressing. This may have been due to the difference in the time of developing the compressive strength that affected the creep of concrete, which resulted as KS followed the compress strength expression of ACI instead of that of CEB-FIP. On the other hand, the analytical results based on the ACI standard were slightly lower than those based on KS or CEB-FIP, indicating a long-term prestress loss.

On the other hand, in the MIDAS analysis program or in general numerical calculations, the wedge slip was assumed to be 3 to 6 mm for calculating the amount of immediate prestress loss generated at the anchorage. Because the total length of the specimen was very short (6350 mm) in this study, a large amount of immediate prestress loss was expected at the anchorage. Therefore, the wedge slip was set to 6 mm. According to the results of the finite-element analysis, the amount of immediate loss occurring at the anchorage was 14.62 kN. However, when a prestress force was applied to the actual specimens, it was reduced from 184.1 kN to 132.7 kN in the composite specimen, and from 179.5 kN to 128.3 kN in the non-composite specimen. This indicated that the immediate prestress

loss while removing the hydraulic jack was significantly larger than the theoretical values based on the analysis, at about 51.2 kN to 51.4 kN. In general, the immediate prestress loss tends to become larger as the length of the specimen becomes shorter. When removing the hydraulic jack, the wedge must be pushed from the hydraulic jack itself to the end to fix the wedge of the anchorage well. Nevertheless, the performance of the hydraulic jack itself may not have supported this. Accordingly, in order to compare the trend of long-term prestress loss, a method was selected to match the analysis results with the experimental results with respect to the prestress force values immediately after loss compared to the initial prestress force. The trends of the changes in long-term prestress loss identified using this method were then classified according to those in the composite and non-composite specimens and are shown in Figures 17 and 18 below.

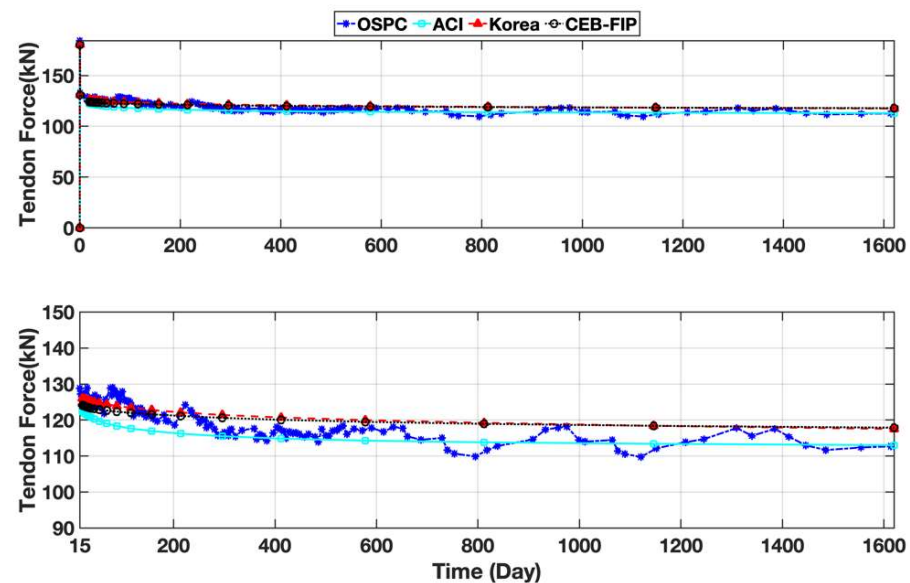


Figure 17. Comparison of long-term prestress loss in composite specimens.

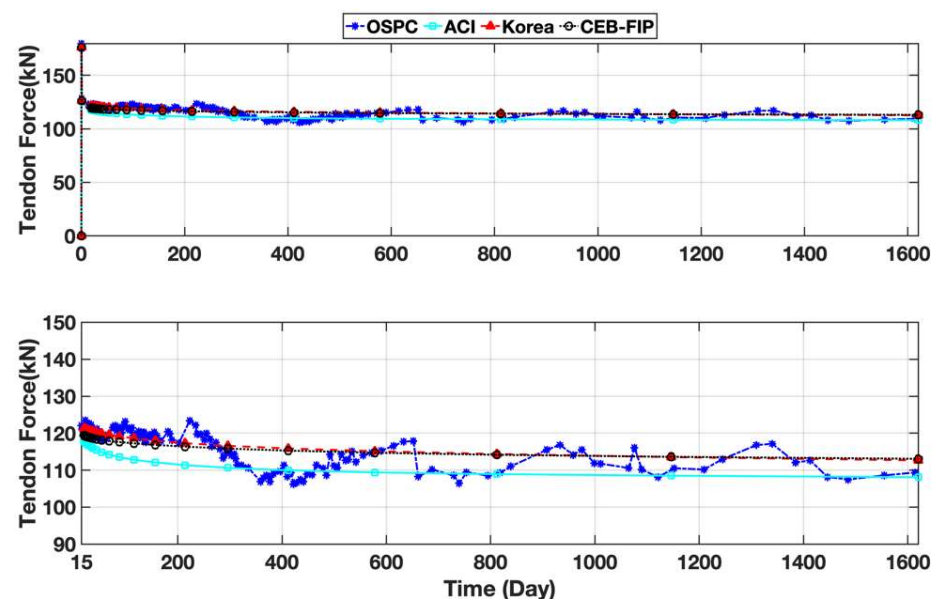


Figure 18. Comparison of long-term prestress loss in non-composite specimens.

As shown in the graph, the results based on KS and CEB-FIP initially appeared to follow a trend that was similar to that of the experimental results in both composite and non-

composite specimens up to about Day 200. After Days 300 and 400, the analytical results based on the ACI standard started to show a trend similar to that of the experimental results in the composite specimen. Even until after Day 1600, the change stayed in between the maximum and minimum values of the data obtained from actual experimental specimens. On the other hand, for non-composite specimens, the analytical results based on the ACI standard were maintained at a low level close to the minimum values, compared to the experimental data. The analytical results based on the KS and CEB-FIP standards were maintained in between the maximum and minimum values of the experimental data. Nevertheless, the difference among the analytical results based on each standard of ACI, KS, and CEB-FIP was about 5 kN, which was only about 3.8% compared to 130 kN, which was the prestress force that was actually introduced. Despite the slight difference in the pattern of prestress loss in the early and late stages, there appeared to be no difficulty in interpreting the long-term prestress loss. However, in actual structures, it is difficult to assess the state based only on analytical values, and sudden damage may occur owing to unexpected external factors. Therefore, it will be necessary to prepare a method for the long-term monitoring of the prestress force, such as the OSPC strand, for PSC structures. The use of the OSPC strand developed in this study enables the stable measurement of the prestress force change in a PSC structure over a long period of time throughout the lifespan of the structure from initial prestressing. As the OSPC strand can immediately detect any change in the prestress force due to sudden structural damage, it is expected to contribute to the effective maintenance of the structure.

4. Conclusions

In this study, a PC strand with an embedded FBG fiber sensor (optical sensor PC strand; OSPC strand) was developed and the tensile strength was determined, which was followed by tensile strength, creep, and relaxation tests. The following conclusions were made by performing long-term measurement of prestress force on the PSC structure for more than 1600 days and by comparing the experimental results with the analytical results obtained in the finite-element analysis.

(1) Tensile test results indicated that prestress force measurement was performed smoothly from the elastic section to the fracture seed using the OSPC strand developed in this study, and the ultimate strength of the OSPC strand was about 2200 MPa, demonstrating a performance that is similar to or better than a general PC strand at 1860 MPa.

(2) As a result of carrying out the creep test, to keep the load constant, and the relaxation test, to keep the displacement constant, for more than 1000 h, the long-term performance of the OSPC strand alone was also superior to that of the general PC strand.

(3) From the results of measuring the change in prestress force for more than 1600 days after manufacturing a PSC beam specimen by installing an OSPC strand and introducing prestress force, the change in the prestress force was well represented according to the change in the external temperature. Furthermore, considering the properties of the optical fiber sensor, which was significantly affected by temperature, separate test specimens were produced by being divided into composite and non-composite specimens depending on whether the optical fiber sensor was embedded in concrete, and experiments were performed by varying the temperature to calculate the coefficient of thermal expansion for each case.

(4) By performing finite-element analyses, the long-term change in prestress force according to standards such as ACI, CEB-FIP, and KS was numerically expressed over a long period of time, and the suitability was determined by comparing the analytical results with the prestress force data of the actual beam specimens, considering the thermal expansion coefficient.

Long-term performance verification of the OSPC strand was completed, and the tension of the PC strand inside an actual structure was efficiently measured. This will enable the efficient maintenance of PSC structures.

Author Contributions: Conceptualization, S.-T.K., Y.-H.P. and S.S.; Performing experiments, C.-H.Y., finite-element analysis and data analysis, Y.-S.P.; writing—original draft preparation, S.-T.K. All authors have read and agree to the published version of the manuscript.

Funding: This research was supported by a grant from a Strategic Research Project (Project No. 20210177-001) funded by the Korea Institute of Civil Engineering and Building Technology.

Institutional Review Board Statement: Not applicable.

Informed Consent Statement: Not applicable.

Data Availability Statement: Data sharing not applicable.

Conflicts of Interest: The authors declare no conflict of interest.

References

1. Fu, D.; Guo, H.; Cheng, X.; Luo, B.; Rao, X. Working stress measurement of prestressed anchor cables: Detection mechanism and experimental study of lift-off test. *Rock Soil Mech.* **2012**, *33*, 2247–2252.
2. Cho, S.; Yim, J.; Shin, S.W.; Jung, H.-J.; Yun, C.-B.; Wang, M.L. Comparative Field Study of Cable Tension Measurement for a Cable-Stayed Bridge. *J. Bridg. Eng.* **2013**, *18*, 748–757. [CrossRef]
3. Park, S.-Y.; Lee, S.; Cho, W. Improvement of lift-off tests via field evaluation of residual load in ground anchor. *J. Korean Geotech. Soc.* **2019**, *35*, 43–51.
4. Ahmad, I.; Suksawang, N.; Sobhan, K.; Corven, J.A.; Vallier, R.; Sayyafi, E.A.; Pant, S. Developing Guidelines for Epoxy Grout Pourback Systems for Controlling Thermal/Shrinkage Cracking at Post-Tensioning Anchorages: Full-Scale Testing and Numerical Analysis. *Transp. Res. Rec.* **2018**, *2672*, 34–43. [CrossRef]
5. SMFMC. *Synthesis Report: Academic Service Contract Related with Maintenance of PSC Box Girder Bridges in Seoul Jurisdiction-Corrosion Investigation of Bonded External Tendons in JeongReung Creek Overpass*; Seoul Metropolitan Facilities Management Corporation (SMFMC): Seoul, Korea, 2018. (In Korean)
6. GeoEngineer. New Design for Genoa's Collapsed Morandi Bridge. 2019. Available online: <https://www.geoengineer.org/news/new-design-for-genoa-collapsed-morandi-bridge> (accessed on 24 January 2019).
7. Kwahk, I.; Park, K.-Y.; Choi, J.-Y.; Kwon, H.; Joh, C. Non-Destructive Evaluation for Sectional Loss of External Tendon of Prestressed Concrete Structures Using Total Flux Leakage. *Appl. Sci.* **2020**, *10*, 7398. [CrossRef]
8. Sumitro, S.; Jarosevic, A.; Wang, M. Elasto-Magnetic Sensor Utilization on Steel Cable Stress Measurement. In Proceedings of the The First fib Congress, Concrete Structures in the 21st Century, Osaka, Japan, 13–19 October 2002; pp. 13–19.
9. Ma, G.; Du, Q. Structural health evaluation of the prestressed concrete using advanced acoustic emission (AE) parameters. *Constr. Build. Mater.* **2020**, *250*, 118860. [CrossRef]
10. Nair, A.; Cai, C.S. Acoustic emission monitoring of bridges: Review and case studies. *Eng. Struct.* **2010**, *32*, 1704–1714. [CrossRef]
11. Zhang, L.; Qiu, G.; Chen, Z. Structural health monitoring methods of cables in cable-stayed bridge: A review. *Measurement* **2021**, *168*, 108343. [CrossRef]
12. Calabrese, L.; Campanella, G.; Proverbio, E. Identification of corrosion mechanisms by univariate and multivariate statistical analysis during long term acoustic emission monitoring on a pre-stressed concrete beam. *Corros. Sci.* **2013**, *73*, 161–171. [CrossRef]
13. Silva, K.; Silva, F.; Mahfoud, T.; Khelidj, A.; Brientin, A.; Azevedo, A.; Delgado, J.; de Lima, A. On the Use of Embedded Fiber Optic Sensors for Measuring Early-Age Strains in Concrete. *Sensors* **2021**, *21*, 4171. [CrossRef] [PubMed]
14. Zhang, S.; Liu, H.; Coulibaly, A.A.S.; DeJong, M. Fiber optic sensing of concrete cracking and rebar deformation using several types of cable. *Struct. Control Health Monit.* **2021**, *28*, e2664. [CrossRef]
15. Alwis, L.S.; Bremer, K.; Roth, B. Fiber Optic Sensors Embedded in Textile-Reinforced Concrete for Smart Structural Health Monitoring: A Review. *Sensors* **2021**, *21*, 4948. [CrossRef] [PubMed]
16. Korea Institute of Civil Engineering and Building Technology. *Development of Smart Prestressing and Monitoring Technologies for Prestressed Concrete Bridges*; Korea Institute of Civil Engineering and Building Technology: Goyang, Korea, 2015.
17. Korean Agency for Technology and Standards. *Uncoated Stress-Relieved Steel Wires and Strands for Prestressed Concrete (KS D 7002)*; Korean Agency for Technology and Standards: Daejeon, Korea, 2011. (In Korean)
18. Kim, S.T.; Yoon, H.; Park, Y.-H.; Jin, S.-S.; Shin, S.; Yoon, S.-M. Smart Sensing of PSC Girders Using a PC Strand with a Built-in Optical Fiber Sensor. *Appl. Sci.* **2021**, *11*, 359. [CrossRef]
19. Sung, H.-J.; Kim, Y.-S.; Kim, J.-M.; Park, G.-H. Temperature Compensation of Optical FBG Sensors Embedded Tendon for Long-term Monitoring of Tension Force of Ground Anchor. *J. Korean Geotech. Soc.* **2012**, *28*, 13–25. [CrossRef]
20. He, J.; Zhou, Z.; Ou, J. Simultaneous measurement of strain and temperature using a hybrid local and distributed optical fiber sensing system. *Measurement* **2014**, *47*, 698–706. [CrossRef]
21. Magura, D.D.; Sozen, M.A.; Siess, C.P. *A study of Stress Relaxation in Prestressing Reinforcement*; University of Illinois Engineering Experiment Station, College of Engineering: Champaign, IL, USA; University of Illinois at Urbana-Champaign: Champaign, IL, USA, 1962.